



Investigation of Electrochemical and Morphological Properties of Mixed Matrix Polysulfone-Silica Anion Exchange Membrane

Khoiruddin & I.G. Wenten*

Department of Chemical Engineering, Faculty of Industrial Technology,
Institut Teknologi Bandung, Jl. Ganesha 10, Bandung 40132, Indonesia

*Email: igw@che.itb.ac.id

Abstract. Mixed matrix anion exchange membranes (AEMs) were synthesized using dry-wet phase inversion. The casting solutions were prepared by dispersing finely ground anion-exchange resin particles in N,N-dimethylacetamide (DMAc) solutions of polysulfone (PSf). Subsequently, nanosilica particles were introduced into the membranes. The results show that evaporation time (t_{ev}) and solution composition contributed to membrane properties formation. A longer t_{ev} produces membranes with reduced void fraction inside the membranes, thus the amount of water adsorbed and membrane conductivity are reduced. Meanwhile, the permselectivity was improved by increasing t_{ev} , since a longer t_{ev} produces membranes with a narrower channel for ion migration and more effective Donnan exclusion. The incorporation of 0.5 %-wt nanosilica particles into the polymer matrix led to conductivity improvement (from 2.27 to 3.41 mS.cm⁻¹). This may be associated with additional pathway formation by hydroxyl groups on the silica surface that entraps water and assists ion migration. However, at further silica loading (1.0 and 1.5 %-wt), these properties decreased (to 1.9 and 1.4 mS.cm⁻¹ respectively), which attributed to inaccessibility of ion-exchange functional groups due to membrane compactness. It was found from the results that nanosilica contributes to membrane formation (increases casting solution viscosity then reduces void fraction) and membrane functional group addition (provides hydroxyl groups).

Keywords: *ion exchange membrane; mixed matrix membrane; polysulfone; silica.*

1 Introduction

Extensive application of synthetic ion exchange membranes (IEMs) in many areas have necessitated improvement of their physico-chemical, electrochemical and mechanical properties. Unfortunately, one desirable property is usually achieved at the cost of another parameter [1]. Therefore, the preparation steps are crucially important to obtain membranes with the desired characteristics. Generally, most commercial IEMs can be classified into two major categories, namely homogeneous and heterogeneous membranes [2], with their typical properties and advantages [3,4]. Recently, organic-inorganic

Received July 3rd, 2014, 1st Revision January 5th, 2015, 2nd Revision February 27th, 2015, Accepted for publication November 10th, 2015.

Copyright ©2016 Published by ITB Journal Publisher, ISSN: 2337-5779, DOI: 10.5614/j.eng.technol.sci.2016.48.1.1

materials have attracted growing interest from researchers because a combination of both materials results in better properties. Activated carbon [5], carbon nano-tubes [6], sulfonated mesoporous silica [1], silica [7], and iron-nickel oxide [8] are examples of inorganic materials that have been used as filler for the IEM matrix. The functions of inorganic fillers are to maintain water uptake, increase ion-exchange capacity and conductivity while retaining good mechanical and chemical stability [9]. However, the introduction of an inorganic filler into the polymer matrix should be carefully controlled to obtain a fine distribution of additives inside the membrane.

Employing silica as filler into the polymer matrix, especially nano-sized silica, has been examined in IEMs and proton exchange membranes (PEMs) preparations. Polyvinyl alcohol (PVA) silica anion exchange membranes (AEMs) have been prepared by sol-gel process using PVA and tetraethylorthosilicate (TEOS) [7]. The prepared AEMs exhibited good dimensional stability, more compactness, and good electrochemical properties. However, at a high concentration of TEOS, incomplete hydrolysis of ethyl groups occurred during the sol-gel process, which blocked the proton pathway and thus reduced conductivity [10].

Mixed matrix polysulfone (PSf)-based IEMs have been prepared as hollow fiber [11] and flat sheet membranes [12]. The flat sheet membranes were prepared by dry phase inversion and the PSf membrane showed higher permselectivity than polycarbonate. In this study, PSf-based mixed matrix AEMs were prepared using a combination of dry and wet phase inversion. Moreover, a simple procedure for dispersing silica nanoparticles is introduced. The effects of the preparation procedure and nanosilica content on the membrane characteristics were studied and evaluated. The results are valuable for obtaining membranes with a simple procedure that have reliable properties and can be used for electro-membrane processes.

2 Materials and Method

The mixed matrix AEMs were prepared by solution casting and phase inversion. Prior to the preparation of the solution, ion-exchange resin particles (Amberlite™ IRA 400-Cl, Rohm and Haas Co.) were dried in an oven at 60 °C for 24 hours, then pulverized into fine particles and sieved into the desired mesh size (-325+400). Polymer solution was prepared by dissolving PSf (Udel Polysulfone P-3500 LCD, Solvay Advanced Polymers) into N,N-dimethylacetamide (DMAc) (Shanghai Jingsan Jingwei Chemical Co., Ltd) and stirred until the solution was optically homogeneous. This was followed by dispersing a specific quantity of resin particles as functional groups agents and mixing until homogeneous. The solution was then sonicated and mechanically

stirred for 30 and 15 minutes, respectively. The mixture was then casted onto a glass plate, dried at ambient temperature for a period of time, and immersed in water. The thickness of the membranes was about 0.57 (± 0.3) mm. As the final stage, the membranes were pretreated by immersing in NaOH and NaCl solutions prior to characterization. Meanwhile, for the fabrication of PSf-silica membrane various colloidal silica (from DuPont, nominal size of 12 nm) quantities were dispersed into DMAc and then sonicated to avoid agglomeration and induce fine distribution. The PSf was then dissolved into a DMAc-silica (25 % -wt PSf in DMAc) mixture, followed by the preparation steps as previously explained. Ten minutes of t_{ev} was chosen for dry-wet phase inversion. The membrane preparation conditions are summarized in Table 1.

Water uptake was measured as weight difference between the dried (in oven 60 °C for 24 hours) and wetted membrane as follows:

$$Water\ Uptake\ (\%) = \frac{W_{wet} - W_{dry}}{W_{dry}} \times 100\% \quad (1)$$

where W_{wet} and W_{dry} are the weight of the wetted and dried membrane, respectively. In a similar method, dimensional changes were measured as the difference between wetted and dried state (Δth = thickness change, %; Δl = length change, %; ΔV = volume change = $\Delta(Area \times th)$, %) using a dial thickness gauge, type DT-3701Y from Delta Precision Tools (precision: 0.01 mm). The dimensional changes were calculated using the following equation:

$$\Delta d\ (\%) = \frac{d_{wet} - d_{dry}}{d_{dry}} \times 100\% , \Delta d = \Delta th, \Delta l, \Delta V \quad (2)$$

The membrane potential was evaluated for the equilibrated membrane with an unequal concentration ($C_1 = 0.1$ M and $C_2 = 0.01$ M) of NaCl using a test cell as shown in Figure 1(a). The developed potential across the membrane was measured using a digital multimeter (CM-888D from CADIK). The membrane potential is expressed using the following equation [1]:

$$E_m = \frac{RT}{F} (2t_i - 1) \ln \left(\frac{C_1}{C_2} \right) \quad (3)$$

where R is gas constant, F is Faraday constant, T is an absolute temperature, t_i is the counter-ion transport number. Meanwhile, permselectivity of the membrane is expressed as:

$$P_s = \frac{t_i - t_o}{1 - t_o} \quad (4)$$

where t_o is the counter-ion transport number in free solution (0.6 for Cl⁻, calculated from [7]). In addition, the surface charge density (X) is expressed as a

function of permselectivity (P_s) and mean concentration of electrolyte solution (C_{mean}) as follows [7]:

$$X = \frac{2C_{mean} \cdot P_s}{\sqrt{1 - P_s^2}} \quad (5)$$

The electrical resistance of the equilibrated membrane (R_m) was measured in 0.5 M NaCl solution (25 °C) by supplying a direct current to the test cell, as shown in Figure 1(b). The R_m was calculated using the difference in resistance between the cell (R_{cell}) and the electrolyte solution (R_{sol}), ($R_m = R_{cell} - R_{sol}$). Then, the membrane conductivity (σ , mS.cm⁻¹) was calculated by:

$$\sigma = \frac{L}{R_m \cdot A} \quad (6)$$

where L is the thickness of the membrane and A is the effective area of the membrane.

The structure of the prepared membranes was examined with a scanning electron microscope (SEM) at 500x magnification. Prior to measurement, each membrane was immersed in liquid nitrogen and then cut into specific dimensions.

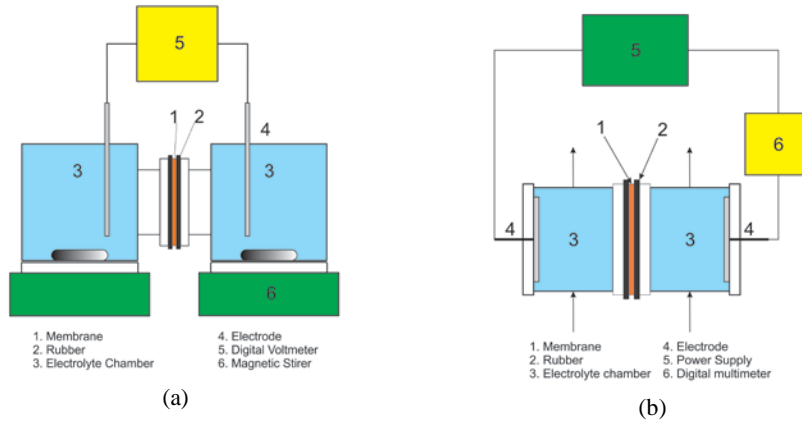


Figure 1 Membrane test cell: (a) membrane potential, and (b) membrane resistance.

3 Results and Discussion

3.1 Preparation Conditions

The preparation conditions and membrane properties are listed in Table 1. Membrane PSf20-1 was formed with a wavy surface and had an optically uneven distribution of polymer and ion exchange particles, so we did not

proceeded with further characterization. This indicates that one minute of evaporation time was not enough to obtain a stable interaction between the polymer matrix and the ion-exchange particles for PSf20-1. Therefore, when the membrane was immersed into the coagulation bath, the solvent–non-solvent exchange between membrane and water (in the coagulation bath) influenced the membrane matrix structure, thus leading to the formation of a waved surface and the release of some resin particles into the coagulation bath.

Table 1 Preparation conditions and membrane properties of mixed matrix AEMs.

Membrane	PSf ^a (%-wt)	Resin ^b (%-wt)	t_{ev}	Water uptake (%)	Swelling State		E_m (mVolt)	t_i
					Δth (%)	Δl (%)		
PSf20-1	20	50	1 min	-	-	-	-	-
PSf20-5	20	50	5 min	146	1.4	0.41	40	0.837
PSf20-10	20	50	10 min	143	1.6	0.53	44	0.871
PSf20-24	20	50	24 hours	103	2.2	0.80	51	0.929
PSf25-1	25	50	1 min	118	1.1	0.55	44	0.871
PSf25-5	25	50	5 min	104	2.2	0.66	47	0.896
PSf25-10	25	50	10 min	83	3.7	1.05	49	0.913
PSf25-24	25	50	24 hours	79	3.6	1.50	53	0.947

^a PSf in PSf-DMAc; ^b ion exchange resin in total solid.

It was noticed that the water uptake decreased with increasing evaporation time (Table 1 and Figure 2). The membrane conductivity showed a trend similar to the water uptake as the water gave more pathways for ion migration (Figure 2). On the other hand, the permselectivity of the membrane increased with decreasing water uptake. It has been reported [1] that IEM porosity can be controlled by adjusting the drying time. More porous membranes are obtained from a shorter t_{ev} . Water adsorption and membrane conductivity are improved with increasing porosity. However, more porous membranes exhibit less effective Donnan exclusion and therefore diminish permselectivity. Table 2 also shows that using the wet phase inversion method resulted in higher conductivity, which can be attributed to increasing porosity. However, the PSf20 membranes showed lower conductivity than those prepared by dry phase inversion in the literature (Table 2). The polymer type also has significant impact on the membrane properties, which can be attributed to characteristics such as degree of hydrophilicity [12]. Moreover, casting methods such as spray coating may result in better distribution of ion-exchange particles inside the polymer matrix [4,13]. These factors may produce membranes with a higher conductivity than that of PSf20. However, when the polymer concentration in the polymer matrix solution was increased from 20 to 25 %-wt, the membrane conductivity and permselectivity became relatively higher compared to those mentioned in the literature (Table 2). These results possibly imply relatively

high ion-exchange functionality associated with the increase of the number of ion exchange particles in the membrane. For example, solution PSf25 had 75 gr of solvent and 25 gr of PSf. Since ion-exchange particles are proportional to polymer, i.e. PSf, the amount of ion-exchange particles was 25 gr. Meanwhile, for PSf20 the same solution contained 80 gr, 20 gr, and 20 gr of solvent, PSf, and ion-exchange particles, respectively. In the phase inversion process, the solvent leaves the solution and porosity is formed inside the membrane film. A high solvent concentration causes a high void volume formation while a high solid concentration causes a high-density membrane. The prepared membrane consists of polymer and ion-exchange particles. Additionally, the electro-chemical properties of the membrane, especially conductivity and permselectivity, mainly depend on ion-exchange groups provided by the ion-exchange particles. Therefore, PSf25 showed better electro-chemical properties than PSf20. However, it should be noted that a combination of good porosity – to achieve a better swelling state – and a high concentration of ion-exchange groups may provide a membrane with better electro-chemical characteristics.

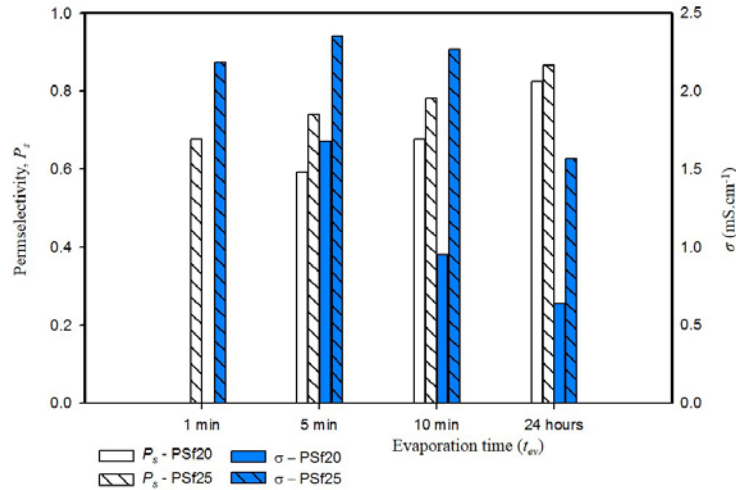


Figure 2 Effect of preparation condition on membrane permselectivity (P_s) and conductivity (σ).

The SEM images show that the membranes were dense for both PSf20 and PSf25 with t_{ev} at 10 minutes (Figure 3). PSf20 should be more porous than PSf25 since PSf20 has more solvent in the casting solution. However, the SEM images show that both types of membrane have a similar structure. On the other hand, PSf25 showed more void volumes around the particles than PSf20. The void volumes provide a wider access channel for ion migration. These void volumes may be formed due to higher solution viscosity, which induces a lower

interaction between the ion-exchange particles and the polymer matrix, even though the particles are still entrapped inside the membrane. Thus, the membrane exhibits better electrochemical characteristics. It may be concluded from the results of the electro-chemical characteristics and morphology of the membranes that the polymer ratio in the solvent contributes to membrane structure formation.

Table 2 Comparison of membrane properties.

Ref.	Polymer	Resin*		Method	Ps	σ (mS/cm)
		Type	Mesh			
[4]	PVC	Cation	-300+400	dry	0.819	1
[12]	PSf	Cation	400	dry	0.818	-
[14]	Polycarbonate	Cation	-200+400	dry	0.853	2
[13]	PVC	Anion	-300+400	dry	-	1
This study						
PSf20-10	PSf	Anion	-325+400	dry-wet	0.677	0.95
PSf20-24	PSf	Anion	-325+400	dry-wet	0.824	0.64
PSf25-10	PSf	Anion	-325+400	dry-wet	0.782	2.27
PSf25-24	PSf	Anion	-325+400	dry-wet	0.866	1.57

*50 %-wt resin in membrane

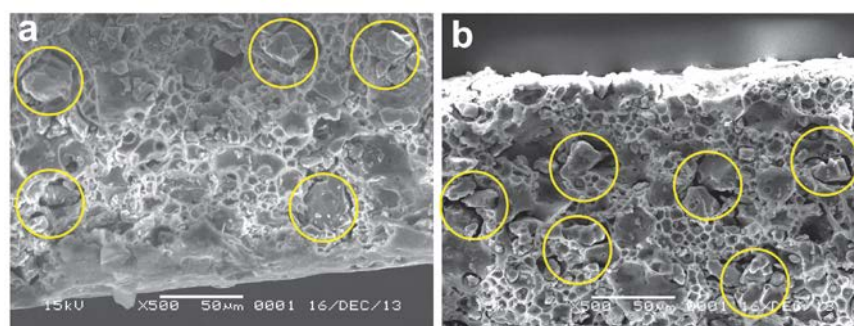


Figure 3 SEM images of (a) PSf20-10 and (b) PSf25-10.

3.2 Effect of Nanosilica

The dry step was introduced to increase solution viscosity prior to precipitation in the coagulation bath (wet phase inversion). At higher viscosity, solvent diffusion is lower and leads to the formation of a thicker top layer [15], which can prevent defects on the membrane surface due to silica-polymer incompatibility. At low silica loading (0,5 %-wt), the conductivity of the membrane was improved, while the permselectivity and transport number were slightly decreased (Figure 4). This possibly implies the improvement of the ion channels provided by the silica. The incorporation of silica into the membrane matrix shows the presence of hydroxyl groups that can entrap water and build pathways for ion diffusion [10]. On the other hand, at higher additive content

(1,0 and 1,5 %-wt) these properties exhibited the opposite trend. It is possible that cavities and voids in the matrix of membrane were reduced, which results in slower ion migration and inaccessibility of functional groups of ion-exchange particles. Therefore, Donnan exclusion becomes more effective, while conductivity becomes depleted. The compactness of the membrane with higher silica loading is shown in Figure 5(b). It is shown that membranes with higher loading silica have a lower water uptake, which corresponds to reduction of the void volume.

It can be observed from the SEM images (Figure 5) that the membranes with higher silica content (1 and 1.5 %-wt) had more void volumes around the particles. However, their polymer matrices were relatively more compact (less porosity), which reduces the pathway for ion migration from solution to particles and from particles to particles. These results are associated with the viscosity of the casting solution. The introduction of silica leads to higher solution viscosity [16]. Membrane solutions cannot be casted into a sheet when incorporating a further increase of silica content (2 and 4 %-wt) into the casting solution, which proves the contribution of silica to solution viscosity (results not shown). An increase in solution viscosity results in improved particle distribution. Meanwhile, a further increase in solution viscosity results in membrane compactness and particle-matrix incompatibility. Thus, from the electro-chemical properties and membrane structures it was found that silica contributed to solution viscosity and membrane functionality (providing hydroxyl groups).

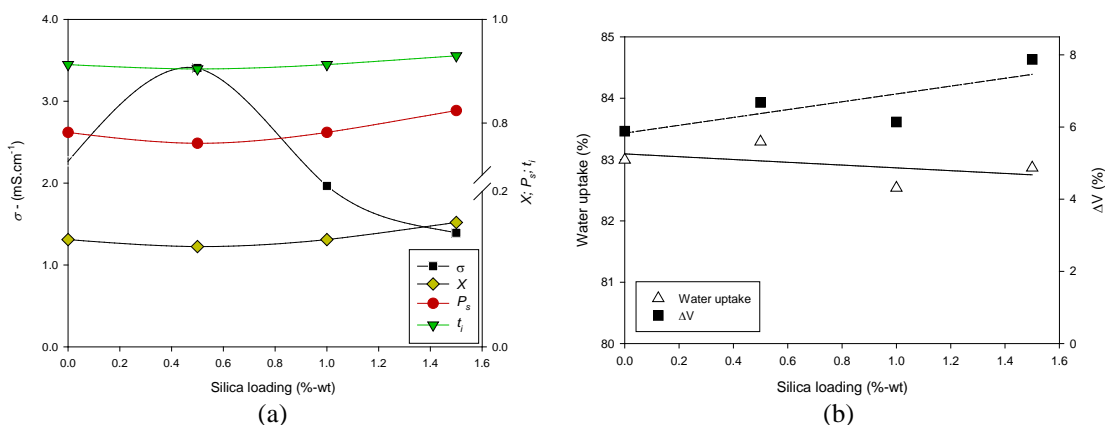


Figure 4 Effect of nanosilica on (a) electro-chemical properties and (b) swelling.

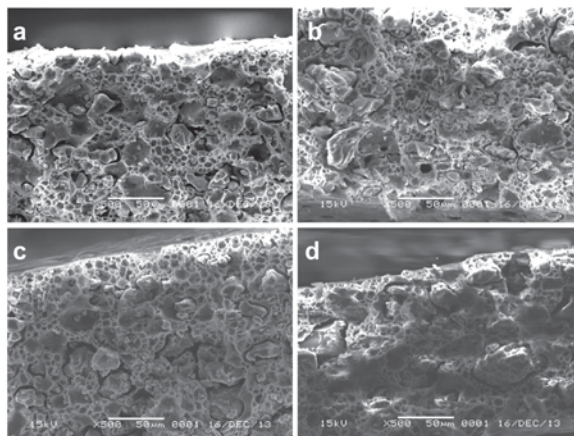


Figure 5 SEM images of PSf-silica AEMs: (a) 0 %-wt, (b) 0.5 %-wt, (c) 1.0 %-wt, and (d) 1.5 %-wt with t_{ev} at 10 min.

4 Conclusion

In summary, preparation condition is a crucial parameter for membrane properties. The results show that evaporation time (t_{ev}) and solution composition contribute to membrane property formation. The incorporation of 0.5 %-wt nanosilica particles into the polymer matrix leads to conductivity improvement (from 2.3 to 3.4 $\text{mS}\cdot\text{cm}^{-1}$). This may be associated with additional channel formation by hydroxyl groups on the silica surface, which entraps water and assists ion migration. However, at further silica loading (1.0 and 1.5 %-wt), these properties are decreased (to 1.9 and 1.4 $\text{mS}\cdot\text{cm}^{-1}$, respectively), which can be attributed to inaccessibility of ion-exchange functional groups due to membrane compactness.

References

- [1] Klaysom, C., Moon, S.H., Ladewig, B.P., Lu, G.Q.M. & Wang, L., *The Effects of Aspect Ratio of Inorganic Fillers on The Structure and Property of Composite Ion-Exchange Membranes*, Journal of Colloid and Interface Science, **363**, pp. 431-439, 2011.
- [2] Kariduraganavar, M.Y., Nagarale, R.K., Kittur, A.A. & Kulkarni, S.S., *Ion-Exchange Membranes: Preparative Methods for Electrodialysis and Fuel Cell Applications*, Desalination, **197**, pp. 225-246, 2006.
- [3] Schauer, J., Llanos, J., Žitka, J., Hnát, J. & Bouzek, K., *Cation-Exchange Membranes: Comparison of Homopolymer, Block Copolymer and Heterogeneous Membranes*, Journal of Applied Polymer Science, **124**, pp. E66-E72, 2012.

- [4] Vyas, P.V., Shah, B.G., Trivedi, G.S., Ray, P., Adhikary, S.K. & Rangarajan, R., *Studies on Heterogeneous Cation-Exchange Membranes, Reactive & Functional Polymers*, **44**, pp. 101-110, 2000.
- [5] Hosseini, S.M., Madaeni, S.S. & Khodabakhshi, A.R., *Preparation and Characterization of ABS/HIPS Heterogeneous Anion Exchange Membrane Filled with Activated Carbon*, *Journal of Applied Polymer Science*, **118**, pp. 3371-3383, 2010.
- [6] Hosseini, S.M., Madaeni, S.S. & Khodabakhshi, A.R., *Preparation and Characterization of PC/SBR Heterogeneous Cation Exchange Membrane Filled with Carbon Nano-tubes*, *Journal of Membrane Science*, **362**, pp. 550-559, 2010.
- [7] Nagaraj, R.K., Shahi, V.K. & Rangarajan, R., *Preparation of Polyvinyl Alcohol-Silica Hybrid Heterogeneous Anion-Exchange Membranes by Sol-Gel Method and Their Characterization*, *Journal of Membrane Science*, **248**, pp. 37-44, 2005.
- [8] Hosseini, S.M., Madaeni, S.S., Heidari, A.R. & Amirimehr, A., *Preparation and Characterization of Ion-selective Polyvinyl Chloride Based Heterogeneous Cation Exchange Membrane Modified by Magnetic Iron-Nickel Oxide Nanoparticles*, *Desalination*, **284**, pp. 191-199, 2012.
- [9] Iojoiu, C., Maréchal, M., Chabert, F. & Sanchez, J-Y., *Mastering Sulfonation of Aromatic Polysulfones: Crucial for Membranes for Fuel Cell Application*, *Fuel Cells*, **5**, pp. 344-354, 2005.
- [10] Ye, G., Hayden, C.A. & Goward, G.R., *Proton Dynamics of Nafion and Nafion/SiO₂ Composites by Solid State NMR and Pulse Field Gradient NMR*, *Macromolecules*, **40**, pp. 1529-1537, 2007.
- [11] Kiyono, R., Koops, G.H., Wessling, M. & Strathmann, H., *Mixed Matrix Microporous Hollow Fibers with Ion-Exchange Functionality*, *Journal of Membrane Science*, **231**, pp. 109-115, 2004.
- [12] Nagaraj, R.K., Shahi, V.K., Thampy, S.K. & Rangarajan, R., *Studies on Electrochemical Characterization of Polycarbonate and Polysulfone Based Heterogeneous Cation-Exchange Membranes*, *Reactive & Functional Polymers*, **61**, pp. 131-138, 2004.
- [13] Vyas, P.V., Shah, B.G., Trivedi, G.S., Ray, P., Adhikary, S.K. & Rangarajan, R., *Characterization of Heterogeneous Anion-Exchange Membrane*, *Journal of Membrane Science*, **187** pp. 39-46, 2001.
- [14] Hosseini, S.M., Madaeni, S.S. & Khodabakhshi, A.R., *Heterogeneous Cation Exchange Membrane: Preparation, Characterization and Comparison of Transport Properties of Mono and Bivalent Cations*, *Separation Science and Technology*, **45**, pp. 2308-2321, 2010.
- [15] Zhang, Z., An, Q., Ji, Y., Qian, J. & Gao, C., *Effect of Zero Shear Viscosity of The Casting Solution on The Morphology and Permeability of*

- Polysulfone Membrane Prepared via The Phase-Inversion Process*, Desalination, **260**, pp. 43-50, 2010.
- [16] Akli, K., Khoiruddin & Wenten, I.G., *Preparation and Characterization of Heterogeneous PVC-silica Proton Exchange Membrane*, Journal of Membrane Science and Research, Articles in Press, 2014, Available online: http://www.msjournal.com/article_10657_0.html.